Available online at www.sciencedirect.com

jmr&t Journal of Materials Research and Technology

www.jmrt.com.br

Original Article

Electrolytic preparation of Mg-Al-La alloys in KCl-$MgCl_2$-AlF_3 molten salts

Pok Nam Jang, Hyon Mo Li, Wen Jae Kim, Song Chol Yun, Gwang Hyok Hwang*

Department of Metallurgical Engineering, Kim Chaek University of Technology, 60 Kyogu, Pyongyang, Democratic People's Republic of Korea

ARTICLE INFO

Article history:
Received 29 August 2018
Accepted 5 September 2019
Available online 4 November 2019

Keywords:
Mg-Al-La master alloy
KCl-$MgCl_2$
KCl-$MgCl_2$-AlF_3 molten salt
$Al_{12}Mg_{17}$ phase
Rare Earth La

ABSTRACT

A KCl-$MgCl_2$-AlF_3 ternary system containing La_2O_3 was investigated for the preparation of Mg-Al-La master alloy by electrodeposition technique. The cyclic voltammetry and chronopotentiometry indicated that the co-reduction of Mg, Al and La occurs at cathode-current densities more negative than $-0.29\,A{\cdot}cm^{-2}$. Lanthanum under-potential deposited on pre-reduced Al and it formed Al-La alloy. Inductively coupled plasma-optical emission spectroscopy (ICP-OES) and X-ray diffraction (XRD) analyses were used to consider the contents of components in the alloy, the supernatant composition of molten salt after dissolution of La_2O_3 and the composition of the alloy, respectively. The galvanostatic electrolysis results showed that the optimum electrolysis conditions were the electrolytic temperature of 800°, the cathode-current density of $6.92\,A{\cdot}cm^{-2}$, and the electrolysis time of 60 min. The XRD and SEM analysis results showed that the main phases of the obtained alloy sample were α-Mg, α-Mg + β-$Al_{12}Mg_{17}$ and α-Mg + $Al_{11}La_3$. The content of magnesium in the Mg-Al-La alloy reach with the increase of the cathode-current density.

Inductively coupled plasma-optical emission spectroscopy (ICP-OES) analyses of Mg-Al-La alloy samples showed that aluminum and Lanthanum contents of Mg-Al-La alloys could be controlled under the several cathode-current density.

1. Introduction

Mg-Al family alloys have a low density and high strength-to-weight, good corrosion resistance as well as are convenient for manufacturing, therefore they are widely used building so on several field [1].

According to the different matrix, the master alloy can be classified into an aluminum-based, a copper-based, an iron-based, a magnesium-based, and a nickel-based master alloy.

Rare earth metal is one kind of important substances to improve the properties of Mg-Al binary alloys [2]. Rare-earth metals have high activity so that a low content of it has high metamorphism effects and impurity refining effects in Al alloy, Mg alloy, and Zn alloy (e.g., AM60 alloy [3], Al-Zn-Mg-Cu based alloy [4–7], Al-7Si-0.7 Mg alloy [8], AZ91 alloy [9] and so on). Rare-earth metal can improve successfully alloy's abilities such as intensity, hardness, conductibility, corrosion

* *Corresponding author.*
E-mail: jbn8011@star-co.net.kp (P.N. Jang).

https://doi.org/10.1016/j.jmrt.2019.09.013

resistance [10–12]. In general, the main production methods of the alloys include mixed melting method, metal heating reduction method, molten salt electrolysis method, and so on.

In the previous works, the reduction of Mg, Li and other ions in LiCl-KCl molten salts was investigated (e.g., and Mg-Li-Zn [13], Mg-Li-Al [14] and Mg-Li [15] alloys on inert electrodes were prepared) and Mg-Al-RE (RE: Ho, Gd, Er, Dy) ternary system [16,17] already was published.

Harata [18] succeeded to get Al-Sc alloy by fused salt electrolysis method. Mikito Ueda [19] obtained Al-Cr-Ni alloy and also Castrillejo [20] made Al-Tm alloy by fused salt electrolysis method. Tao Cheng [21] studied to make Mg-Al-Sc alloy as fused salt electrolysis method in LiF-ScF_3-$ScCl_3$ system.

Zhang [22] studied to make foam of Al-2 wt. % Mg-RE that had comparatively tiny abscess by melt solution foam method.

Han [23] studied to make Mg-Li-Sm alloy in KCl-LiCl-$MgCl_2$-$SmCl_3$-KF system by fused salt electrolysis method. Han [24] made Al-Li-La alloy in LiCl-KCl-$AlCl_3$-La_2O_3 system. However, there is not report on preparation of Mg-Al-La master alloy by fused salt electrolysis method in KCl-$MgCl_2$-AlF_3-(La_2O_3) molten salt.

In this work, the Mg-Al-La master alloy was prepared by fused salt electrolysis in KCl-$MgCl_2$-AlF_3-La_2O_3 molten salts. Electrochemical co-reduction of Mg, Al, and La ions in KCl-$MgCl_2$-AlF_3-La_2O_3 molten salts on Mo electrode is proposed for direct preparation of Mg-Al-La alloys at 800 °C. The microstructure of the obtained alloy sample was analyzed and discussed.

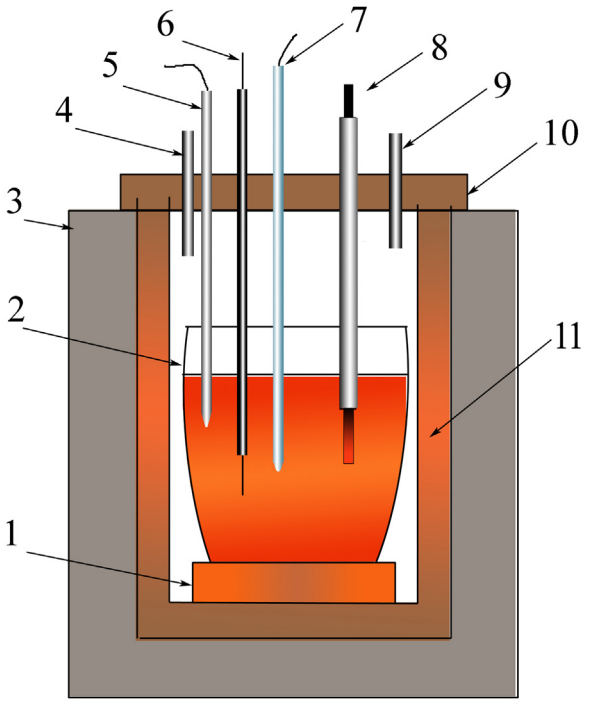

Fig. 1 – Schematic diagram of the molten salt electrolysis. 1-Firebrick base, 2-Graphite crucible, 3-Resistance furnace, 4-Argon inlet, 5-Thermoelectric couple 6-Mo cathode, 7-reference electrode, 8-Graphite rod anode, 9-Gas outlet, 10-Electrolyzer cover, 11-Cylinder pipe.

2. Experimental procedures

2.1. *Preparation of the molten salts*

AlF_3 and La_2O_3 (≧99.0%), $MgCl_2$ and potassium chloride (KCl, 99.9%) were purchased from Sinopharm Chemical Reagent Co., Ltd. (Shanghai, China). All the reagents were dehydrated under vacuum at 673 K (400 °C) for 24 h to remove the moisture before use. The metal molybdenum line was used as the cathode and spectroscopic pure graphite was used as the anode. The manufacturing method of anhydrous AlF_3 is as follows. $AlF_3 \cdot 3H_2O$ and ammonium bifluoride (NH_4HF_2) were mixed to the mass ratio of 7:3 evenly and made vacuum dehydration for two hours at 150 °C and 250 °C each other and constant temperature maintenance for three hours at below 500 °C.

Chloride mixture (KCl:$MgCl_2$ = 50:50 (in mol. %), analytical grade) was melted in graphite crucible placed in a quartz cell inside an electric furnace. Al (III) and La (III) ions were introduced into the bath in the form of dehydrated AlF_3 and La_2O_3 powder. All experiments were performed under an argon atmosphere.

2.2. *Experimental apparatuses*

The schematic diagram of experimental apparatus is shown in Fig. 1.

All potentials were referred to the Ag/AgCl couple.

The working electrode was molybdenum (99.99% purity) wire with a diameter of 1 mm, which was fixed in alundum tube and was polished thoroughly using SiC paper, and then cleaned in the ultrasonic ethanol bath. A spectrally pure graphite rod (d = 6 mm) was used as the counter electrode.

2.3. *Measurement and characterization*

Autolab electrochemical workstation (Metrohm Co., Ltd.) was used for all electrochemical measurements.

ICP-OES (Optima 8300 DV; Perkin Elmer Corp., Waltham, MA) was used for the quantitative analysis of the components contents in the alloy.

X-ray diffraction (XRD; PW3040/60; PANalytical Corp., Almelo, the Netherlands) analysis was used for the qualitative analysis of the Mg-Al-La alloy composition and the supernatant composition of molten salt after dissolution of La_2O_3.

SEM and EDS (JSM-6610A; JEOL Co., Ltd.) analysis was used for the microstructure analysis of Mg-Al-La master alloy.

3. Results and discussion

3.1. *Interaction between the molten salts compositions*

When the content of KCl is 50 mol. %, the compound $KMgCl_3$ exists and its melting point is low comparatively [25]. In the eutectic point neighborhood the composition curve of $MgCl_2$-KCl molten salts is destroyed monotonously [26]. As can be seen from this, the compound $KMgCl_3$ is dissociated into the

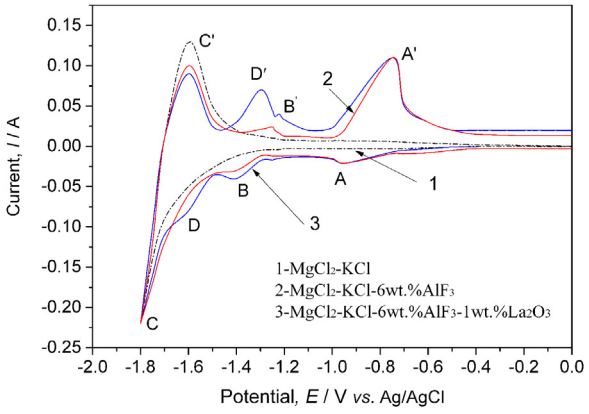

Fig. 2 – Cyclic voltammetry curves of the molten salts on the Mo electrode (S = 0.31 cm^2) at 800 °C with the scanning rate of 100 mV s^{-1}.

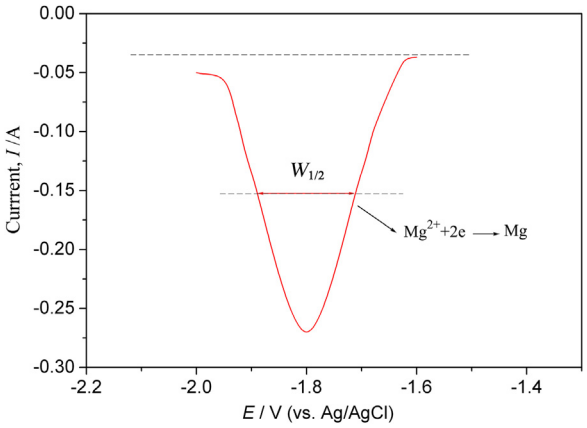

Fig. 3 – Net-current square wave voltammogram for the reduction of Mg^{2+} on Mo electrode in the melt at 800 °C (1073 K): frequency, 20 Hz.

molten salts as following.

$$KMgCl_3 \rightarrow K^+ + MgCl_3^- \rightarrow K^+ + MgCl^+ + 2Cl^- \rightarrow K^+ + Mg^{2+} + 3Cl^- \quad (1)$$

The interaction between the molten salts compositions at 700–850 °C as follows.

$$MgCl_2 + La_2O_3 = 2LaOCl + MgO[Ref.27] \quad (2)$$

$$LaOCl + MgCl_2 = LaCl_3 + MgO[Ref.27] \quad (3)$$

From the above equations, the formed $LaCl_3$ is able to provide La^{3+} in our experimental condition.

The anodic reaction is $2Cl^- - 2e \rightarrow Cl_2$. The formed Cl_2 gas can react with LaOCl on the surface of anode and form CO gas [28].

$$LaOCl + C + Cl_2 = LaCl_3 + CO \quad (4)$$

The cathodic reactions are as follows.

$$Al^{3+} + 3e \rightarrow Al$$

$$Mg^{2+} + 2e \rightarrow Mg$$

$$xAl + La^{3+} + 3e \rightarrow Al_xLa$$

$$xAl + Mg^{2+} + 2e \rightarrow Al_xMg$$

3.2. *Cyclic voltammetry curve in KCl-$MgCl_2$-AlF_3-La_2O_3 system at Mo electrodes*

To study the mechanism of electrodeposition, cyclic voltammetry measurement was performed as shown in Fig. 2. The cyclic voltammetry curves were scanned for the Mo cathode (S = 0.31 cm^2) from −1.8 V (vs. Ag/AgCl) at 800 °C with scanning rate of 100 mV·s^{-1}.

All potentials were referred to the Ag/AgCl couple.

As shown in Fig. 2, a pair of oxidation-reduction signals (C' and C) appeared in the curve-1, which corresponds to the oxidation-reduction process of Mg.

After adding of AlF_3 into the $MgCl_2$-KCl system, the other peaks (A' and A) and (B' and B) appeared on curve 2. The peak potential of A is about −0.95 V. (vs. Ag/AgCl) The peak A was corresponding to deposition of Al on electrode surface. This peak potential of A is similar to the peak in Ref. [24]. The pair of signals (B' and B) correspond to oxidation-reduction signals for alloy Al_xMg. Curve 3 is cyclic voltammetry curve in system KCl-$MgCl_2$-AlF_3-La_2O_3.

As known from curve 3, after adding 1 wt.% La_2O_3 in the molten salt, the another oxidation-reduction signal (D' and D) was observed. This would be the signal related with production of compounds.

The peak D that was detected at −1.55 V corresponds to the formation of Al_xLa. The reduction signal D for Al_xLa also could be concordant with the signal for Al_xLa reported by Han et al. [24] in LiCl-KCl-$AlCl_3$-La_2O_3 system.

3.3. *Square wave voltammetry for the KCl-$MgCl_2$-AlF_3-La_2O_3 system on the Mo cathode*

The square wave voltammogram (SWV) is another analytical technique to determine the electron transfer number (n) in an electrode process. The width of the half-peak, $W_{1/2}$, depends on n and on the temperature (T) as follows [29].

$$W_{1/2} = 3.52RT/nF \quad (5)$$

Using the half peak ($W_{1/2}$) of Gaussian wave, the number of exchanged electrons can be calculated.

The relationship between the half peak of Gaussian wave and the number of exchanged electrons is the same as the Eq. (5).

Fig. 3 shows the square wave voltammogram (SWV) for the reduction of Mg^{2+} on the Mo cathode.

By measuring $W_{1/2}$ of this peak and using the Eq. (5), the average number of electrons transferred was calculated as $n = 1.983$. The number of electrons transferred is close to two.

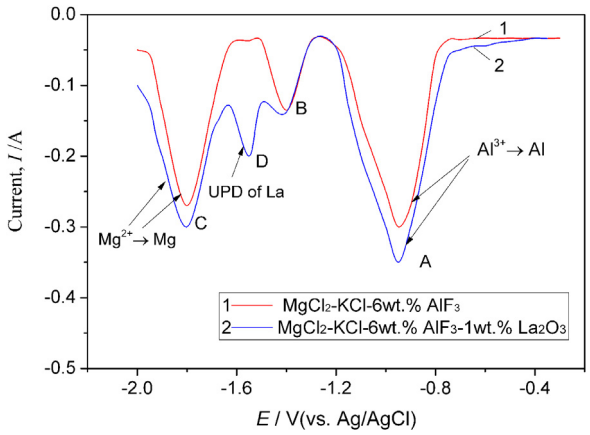

Fig. 4 – Net-current square wave voltammogram on Mo electrode (S = 0.31 cm^2) in KCl-$MgCl_2$ system at 1073 K (800 °C) and 20 Hz.

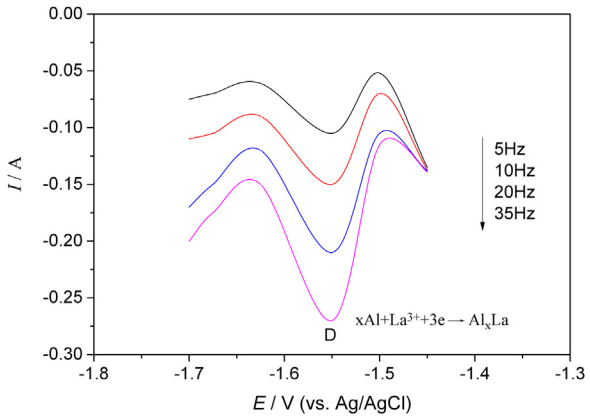

Fig. 5 – Typical square wave voltammograms for the reduction of La on Mo electrode (S = 0.31 cm^2) in KCl-$MgCl_2$-AlF_3-La_2O_3 at 1073 K (800 °C) and 5–35 Hz.

Fig. 4 shows the SWVs for the reduction of Mg, Al and La on the Mo electrode in the KCl-$MgCl_2$ molten salts at frequency of 20 Hz.

In curve 1 (Fig. 4), there were three peaks A, B and C corresponding to the deposition of Al and Mg on the Mo electrode. After adding 1 wt.% La_2O_3 in the molten salt, the another peak D appeared in curve 2. In consideration with Fig. 2, the cathodic peak D was identified as the reduction of La (III) ion on Al substrate forming intermetallic compounds.

Fig. 5 shows the results observed by the square wave voltammetry corresponding to the mentioned peak D on Mo electrode in KCl-$MgCl_2$-AlF_3-La_2O_3 at the various frequencies and 1073 K (800 °C). The scan frequency varied from 5 to 35 Hz. As shown in Fig. 5, the square wave voltammograms exhibit the peak current in the same potential range, and then, the peak current is increasing with the increase of the scan frequency.

The average number of electrons transferred was calculated as $n = 2.94$ by measuring $W_{1/2}$ and using Eq. (5). The number of electrons transferred is close to 3, which confirm that the reduction La(III)→La(0) on Al substrate is a single step with three electrons exchanged.

3.4. *Chronopotentiometry of KCl-$MgCl_2$-AlF_3-La_2O_3 system at Mo electrodes*

Chronopotentiometry was employed to further investigate the electrochemical formation of Mg-Al-La alloys via co-reduction of Mg, Al and La. Fig. 6 presents that the chronopotentiograms were measured in KCl-$MgCl_2$-6 wt.% AlF_3-1 wt.% La_2O_3 melts at different current densities. The first plateau marked by curve (1) at the cathode current up to 20 mA (i = 0.06 A·cm^{-2}) is associated with the reduction of Al (III) ion.

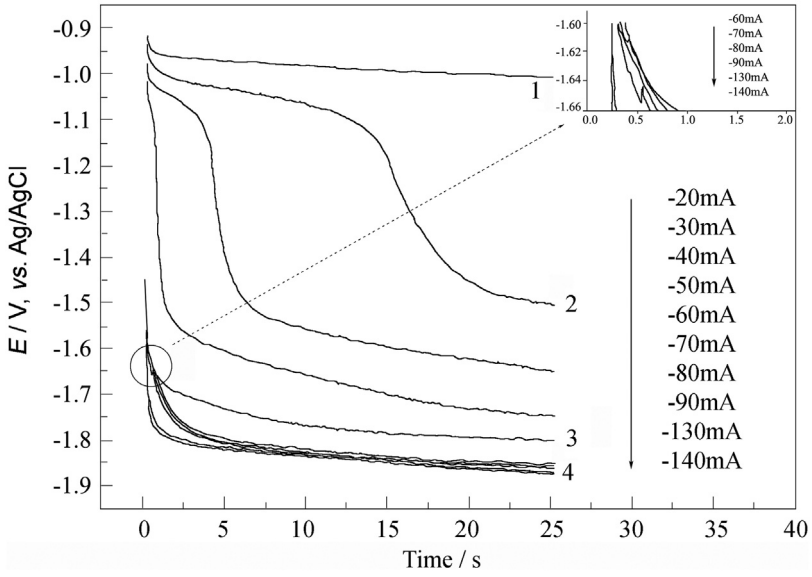

Fig. 6 – Chronopotentiograms at different currents on the Mo electrode (S = 0.31 cm^2) in KCl-$MgCl_2$- AlF_3-La_2O_3 molten salt at 800 °C.

Table 1 – ICP-OES analysis results of some alloys prepared under the different electrolysis conditions from KCl-$MgCl_2$-AlF_3-1 wt.%La_2O_3 molten salt.

№	Tem. (°C)	Time (min)	i (A·cm^{-2})	Al (wt. %)	La (wt. %)	Mg (wt. %)	Current efficiency (%)
1	700	60	6.92	6.90	2.64	Bal.	42.45
2	750	60	6.92	12.88	2.99	Bal.	51.25
3	800	30	6.92	62.01	1.57	Bal.	47.89
4	800	60	3.46	81.10	7.38	Bal.	53.24
5	800	60	5.19	60.30	5.05	Bal.	57.4
6	800	60	6.92	27.00	3.17	Bal.	71.2
7	800	90	6.92	9.88	4.20	Bal.	62.88
8	800	120	6.92	8.17	2.63	Bal.	67.58
9	850	60	6.92	27.10	5.40	Bal.	66.52
10	800	60	8.65	6.57	1.56	Bal.	64.5

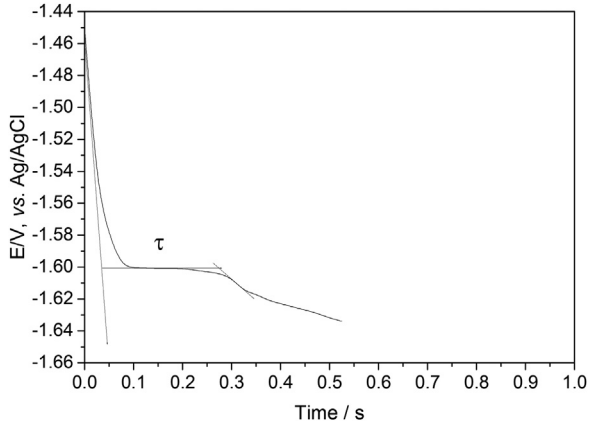

Fig. 7 – Chronopotentiogram of La(III) in KCl-$MgCl_2$-AlF_3-La_2O_3 (CLa(III) = 1.23 × 10^{-4} mol/cm^3)molten salt at 800 °C. I = 80 mA (i = 0.258 A/cm^2).Working electrode area of 0.31 cm^2. Reference electrode: Ag/AgCl.

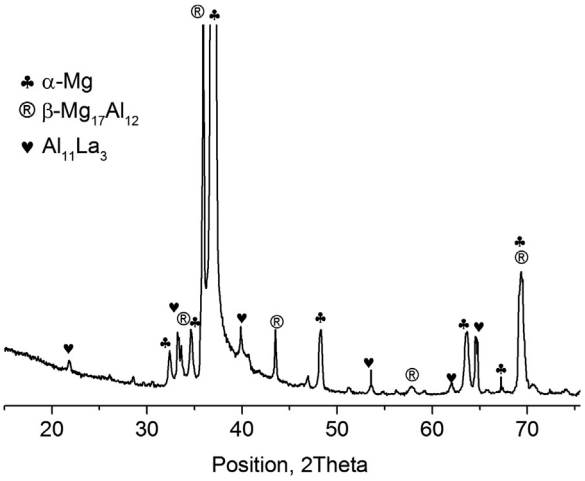

Fig. 8 – XRD pattern of the Mg-Al-La alloy after electrolysis from KCl-$MgCl_2$-6 wt.%AlF_3-1 wt.%La_2O_3 molten salt at 800 °C for 60 min (cathode-current density of 6.92 A·cm^{-2}).

Under the applied current 30 mA (i = 0.10 A·cm^{-2}) and more, the plateaus marked by curve (2) are associated with the formation of Al_xMg.

When the applied current is 60 mA (i = 0.194 A·cm^{-2}) to 80 mA (i = 0.258 A·cm^{-2}), the curve (3) is corresponding to the formation of Al_xLa.

At the cathode current higher than 90 mA (i = 0.29 A·cm^{-2}), the curve (4) is ascribed to the deposition of Mg on Mo electrodes.

According to Sand' s law, the Eq. (6) demonstrates the relationship between the current density and the transition time [29,31].

$$I\tau^{1/2} = 0.5nFAC_0D^{1/2}\pi^{1/2} \quad (6)$$

where I is the current, A; τ is the transition time, s; C_0 C_0^* is the concentration of La^{3+} ion, mol/cm^3; n is the electron charged number; F is the Faraday constant (96500C/mol); A is electrode area (0.31 cm^2); D is diffusion coefficient, cm^2/s. The transition time was determined by measuring the duration of the first part in the chronopotentiograms according to methodology indicated in Ref. [30]. The chronopotentiogram presented in Fig. 7 exhibits an transition time (τ = 0.24 s). By using the average value $I\tau^{1/2}$, the diffusion coefficient was calculated using the Eq. (6) as 1.82 × 10^{-5} cm^2/s (±10 pct).

3.5. *Galvanostatic electrolysis of Mg-Al-La alloys and characterization*

Cyclic voltammetry curves and chronopotentiograms show that electrochemical co-reduction occurred when the potentials are negative than −1.8 V or the cathode current densities are negative than −0.29 A·cm^2. The limiting cathode-current density is too small to deposit enough alloys in a short time for SEM and XRD analyses. So the galvanostatic electrolysis were carried out at more negative current densities in KCl-$MgCl_2$-6 wt. %AlF_3-1 wt. %La_2O_3 molten salts with different electrolysis temperature and electrolysis time, using a molybdenum electrode.

The current efficiency is able to calculate according to following equation. [23]

$$\eta = \frac{Q_{Mg} + Q_{Al} + Q_{La}}{I \cdot t} \quad (7)$$

where Q_{Mg}, Q_{Al} and Q_{La} are the electrical quantities of the deposited Mg, Al and La, respectively, A·h ; t is the electrolysis time, h; I is current intensity, A.

According to Faraday's Law, $Q = nzF$.

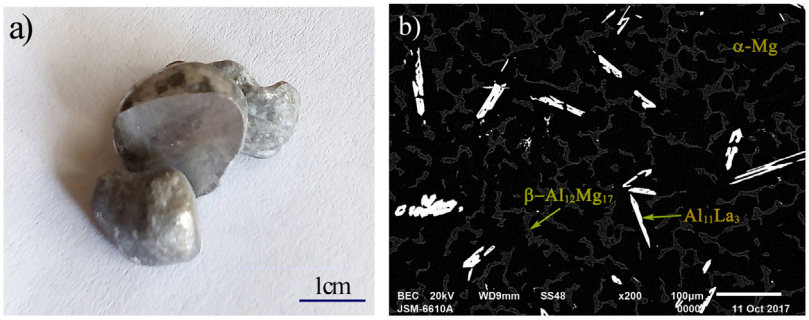

Fig. 9 – (a) Sample image and (b) Microstructure of the Mg-Al-La alloy obtained by galvanostatic electrolysis from KCl-$MgCl_2$-6 wt.%AlF_3-1 wt.%La_2O_3 molten salt at 800 °C for 60 min. (cathode-current density of 6.92 A·cm^{-2}).

Where: *n* is the amount of the deposited metal, mol; *z* is number of the transferred electrons; *F* is Faraday's constant, 26.801 A·h/mol.

ICP-OES analyses of samples obtained by galvanostatic electrolysis are listed in Table 1. Under the same electrolysis time, with increase of the cathode current density, the content of Mg among the alloy was increased continuously, and then the contents of Al and La were decreased. The contents of Al and La in the alloy are increased while the content of Mg in the alloy is continuously decreased with the increase of electrolysis temperature. At the same electrolysis temperature, the content of Mg in the alloy was continuously increased and La content was decreased with the increases of cathode-current density and electrolysis time.

Fig. 8 shows the XRD pattern of Mg-Al-La alloy sample obtained by galvanostatic electrolysis from KCl-$MgCl_2$-6 wt.%AlF_3-1 wt.%La_2O_3 molten salt at 800 °C for 60 min under the cathode current density of 6.92 A·cm^{-2}. As shown in Fig. 8, the sample consists of $Al_{11}La_3$, β-$Al_{12}Mg_{17}$ and α–Mg phase. Fig. 9 shows the sample image (a) and microstructure (b) of

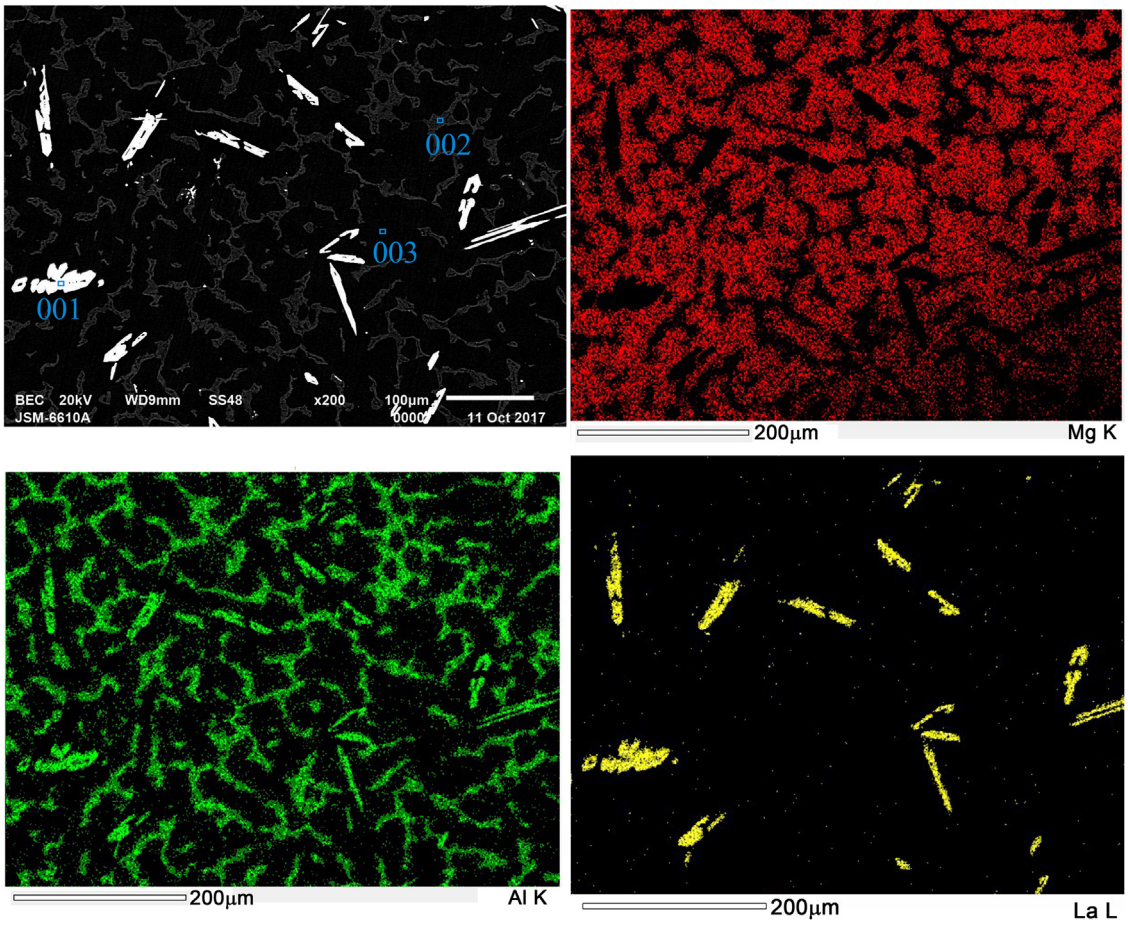

Fig. 10 – EDS mapping analysis of the Mg-Al-La alloy according to Fig. 9(b).

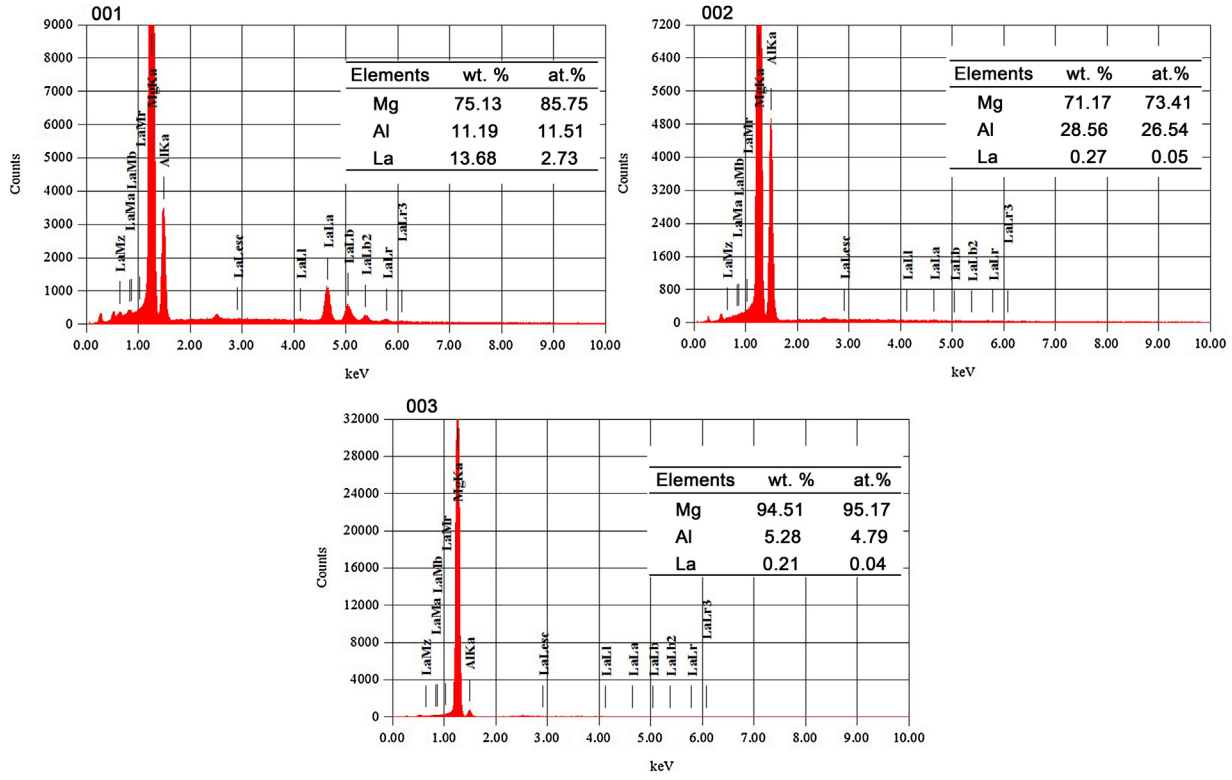

Fig. 11 – Chemical constitutions of the point 001, point 002 and point 003 in Fig. 10 obtained by EDS analysis.

the Mg-Al-La alloy sample obtained by galvanostatic electrolysis from KCl-$MgCl_2$-6 wt.%AlF_3-1 wt.%La_2O_3 molten salt under the electrolysis temperature of 800°, the cathode current density of 6.92 A·cm^{-2} and electrolysis time of 60 min.

Figs. 10 and 11 show the SEM equipped with EDS quantitative analysis applied to figure out the distribution of Mg, Al and La in the Mg-Al-La alloy.

As compared with XRD analysis, the EDS results (Fig. 11) of points 001, 002 and 003 indicate the α-Mg + $Al_{11}La_3$ phase and α-Mg + β-$Al_{12}Mg_{17}$ phase are distributed in Mg-Al-La alloy sample obtained by galvanostatic electrolysis from KCl-$MgCl_2$-6 wt.%AlF_3-1 wt.%La_2O_3 molten salt at 800 °C for 60 min. The form of the alloy sample phases obtained from the SEM analysis results are in agreement with those observed in Ref. [9]. As shown in Fig. 9, α-Mg + β-$Al_{12}Mg_{17}$ phase is mainly distributed in the grain boundaries.

4. Conclusions

Electrochemical techniques showed that the co-reduction occurred when the current densities are more negative than −0.29 A·cm^{-2}.

Under the conditions having the maximum current efficiency, Mg-Al-La alloys with α–Mg, β-$Al_{12}Mg_{17}$ phase and $Al_{11}La_3$ phase were successfully prepared via galvanostatic electrolysis co-reduction of Mg, Al and La on inert molybdenum electrodes in KCl-$MgCl_2$-AlF_3-La_2O_3 molten salts. An analysis of microstructures shows that the banding eutectic structure of (α-Mg + $Al_{11}La_3$) phase and the flaky crystal of (α-Mg + β-$Al_{12}Mg_{17}$) phase are distributed in Mg-Al-La alloy sample obtained by galvanostatic electrolysis from KCl-$MgCl_2$-6 wt.%AlF_3-1 wt.%La_2O_3 molten salt at 800 °C for 60 min (cathode-current density of 6.92 A·cm^{-2}). The contents of Al and La in the alloy are increased while the content of Mg in the alloy is decreased continuously with the increase of electrolysis temperature. At the same electrolysis temperature, the content of Mg in the alloy was increased continuously and La content was decreased with the increases of cathode-current density and electrolysis time.

Conflicts of interest

The authors declare no conflicts of interest.

Acknowledgements

The authors would like to thank the support from the Department of Metallurgical Engineering, Kim Chaek University of Technology.

The authors acknowledge the great help on the offering of scientific data for the alloy preparation by scientific research organization workers and famous professors, Kim Chaek University of Technology.

REFERENCES

[1] Yang Z, Li JP, Zhang JX, et al. Review on research and development of magnesium alloys. Acta Metall Sin 2008;21:313–28.

[2] Lu YZ, Wang QD, Zeng XQ, et al. Mater Sci Eng A 2000;278:66.
[3] Zhang J, Wang S, Zhang J, et al. Effects of Nd on microstructures and mechanical properties of AM60 magnesium alloy in vacuum melting. Rare Met Mater Eng 2009;38(7):1141–5.
[4] Lai J, Jiang R, Liu H, et al. Influence of cerium on microstructures and mechanical properties of Al-Zn-Mg-Cu alloys. J Cent South Univ 2012;19(4):869–74.
[5] Zang Z, Chen K, Fang H, et al. Effect of Yb addition on strength and fracture toughness of Al-Zn-Mg-Cu-Zr aluminum alloy. Trans Nonferrous Met Soc China 2008;18(5):1037–42.
[6] Fang HC, Chao H, Chen KH. Effect of Zr, Er and Cr additions on microstructures and properties of Al–Zn–Mg–Cu alloys. Mater Sci Eng A 2014;610:10–6.
[7] Zou L, Pan Q, He Y, et al. Effect of minor Sc and Zr addition on microstructures and mechanical properties of Al-Zn-Mg-Cu alloys. Trans Nonferrous Met Soc China 2007;17(2):340–5.
[8] Qiu H, Yan H, Hu Z. Effect of samarium (Sm) addition on the microstructures and mechanical properties of Al-7Si-0.7Mg alloys. J Alloys Compd 2013;567:77–81.
[9] Nami B, Razavi H, Mirdamadi S, et al. Effect of Ca and rare earth elements on impression creep properties of AZ91 magnesium alloy. Metall Mater Trans A 2010;41:1973–82.
[10] Li H, Sun Y, Bin J, et al. Effect of cerium on as-cast microstructure and properties of heat-resistant aluminum conductor. J Central South Univ (Sci Technol) 2011;42(10):3026–32.
[11] Yuan W, Liang Z, Zhang C, et al. Effects of La addition on the mechanical properties and thermal-resistant properties of Mg-Al-Si-Zr alloys based on AA 6201. Mater Des 2012;34:788–92.
[12] Zhou WW, Cai B, Li WJ, et al. Heat-resistant Al-0.2Sc-0.04Zr electrical conductor. Mater Sci Eng A 2012;552:353–8.
[13] Yan YD, Zhang ML, Xue Y, Han W, Cao DX, Wei SQ. Study on the preparation of Mg-Li-Zn alloys by electrochemical codeposition from LiCl-KCl-MgCl2-ZnCl2 melts. Electrochim Acta 2009;54:3387–93.
[14] Han W, Chen Q, Ye K, Yan YD, Zhang ML. New preparation of Mg-Li-Al alloys by electrolysis in molten salt. Acta Metall Sin (Engl Lett) 2010;23:129.
[15] Chen Z, Zhang ML, Han W, Hou ZY, Yan YD. Electrodeposition of Li and electrochemical formation of Mg-Li alloys from the eutectic LiCl-KCl. J Alloys Compd 2008;464:174–8.
[16] Cacciamani G, De Negri S, Saccone A, et al. The Al-R-Mg (R=Gd, Dy, Ho) systems. Part II: Thermodynamic modelling of the binary and ternary systems. Intermetallics 2003;11:1135–51.
[17] Cacciamani G, Saccone A, De Negri S, et al. The Al-Er-Mg ternary system Part II: Thermodynamic modeling. J Phase Equilibria Diffus 2002;23(1):38–50.
[18] Harata M, Yakushiji K, Okabe TH. Electrochemical production of Al-Sc alloy in CaCl2-Sc2O3 molten salt. J Alloys Compd 2009;474(1-2):124–30.
[19] Ueda M, Kigawa H, Ohtsuka T. Co-deposition of Al-Cr-Ni alloys using constant potential and potential pulse techniques in AlCl3-NaCl-KCl molten salt. Electrochim Acta 2007;52(7):2515–9.
[20] Castrillejo Y, Fernandez P, Bermejo MR. Electrochemistry of thulium on inert electrodes and electrochemical formation of a Tm-Al alloy from molten chlorides. Electrochim Acta 2009;54(26):6212–22.
[21] Cheng T, Lv Z, Zhai X, et al. Preparation of Mg-Al-Sc Alloys in the System of LiF-ScF3-ScCl3. Chinese Rare Earths 2011;32(1):86–9.
[22] Zhang YM, Chu XM, Hui W, et al. Fabrication of Mg-Al-RE foams and their corrosion resistance properties. Corros Sci 2009;51(6):1436–40.
[23] Han W, Tian Y, Zhang M, et al. Preparation of Mg-Li-Sm alloys by electrocodeposition in molten salt. J Rare Earths 2009;27(6):1046–50.
[24] Han L, Han W, Wang G, et al. Preparation of Al-Li-La alloys by electrochemical codeposition in LiCl-KCl-AlCl3-La2O3 melts. Chinese J Appl Chem 2013;30(6):698–704.
[25] Perry GS, Fletcher H. The magnesium chloride-potassium chloride phase diagram. J Phase Equilibria Diffus 1993;14(2):172–8.
[26] Xie G. Theory and application of molten salt. Beijing: Metallurgical Industry Press; 1998.
[27] Zhang M, Cao P, Han W. Preparation of Mg-Li-La alloys by electrolysis in molten salt. Trans Nonferrous Met Soc China 2012;22:16–22.
[28] Wang S, Li Q, Ye X, Sun Q, et al. Effect of oxide and fluoride addition on electrolytic preparation of Mg—La alloy in chloride molten salt. Trans Nonferrous Met Soc China 2013;23:3104–11.
[29] Bard AJ, Faulkner LR. Electrochemical methods, fundamentals and applications. New York: Wiley; 2000. p. 231–310.
[30] Laity RW, Mclntyre DE. J Am Chem Soc 1965;87:3806–12.
[31] Jain RK, Gaur HC, Welch BJ. J Electroanal Chem (Lausanne) 1977;79:211–36.